

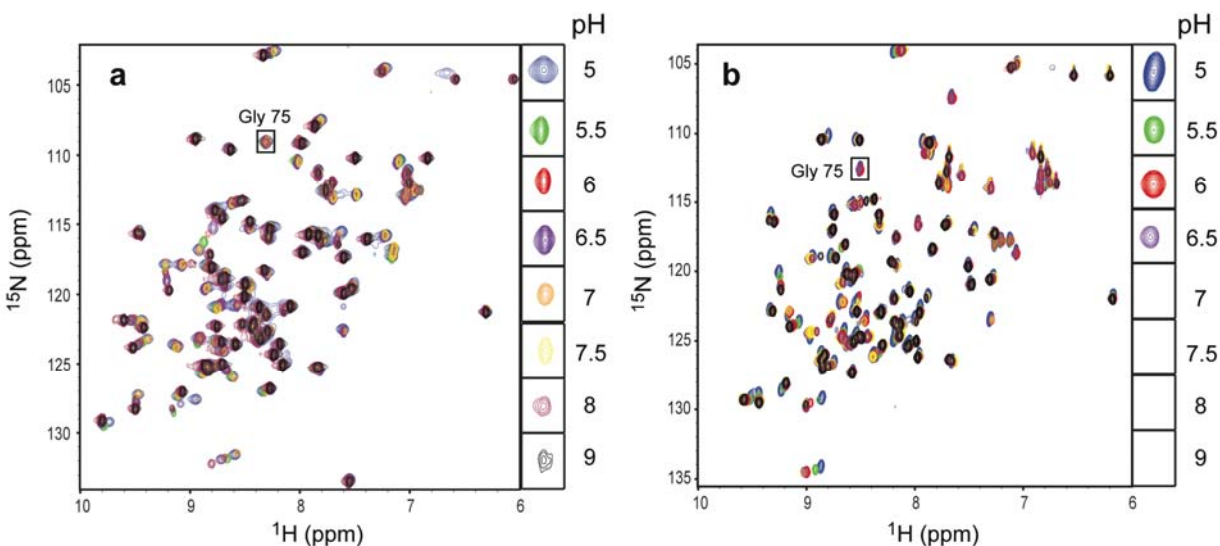
Supporting Material

Site-Resolved Measurement of Water-Protein Interactions by Solution NMR

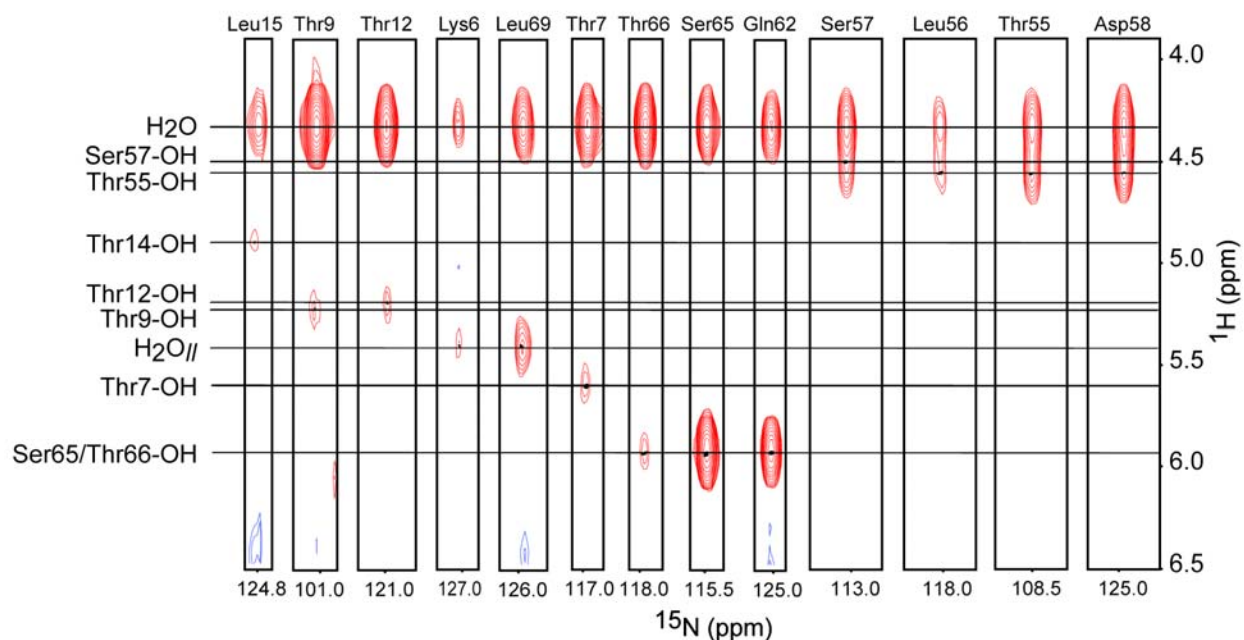
Nathaniel V. Nucci, Maxim S. Pometun and A. Joshua Wand

Department of Biochemistry and Biophysics, University of Pennsylvania, Philadelphia,
Pennsylvania, 19104-6059.

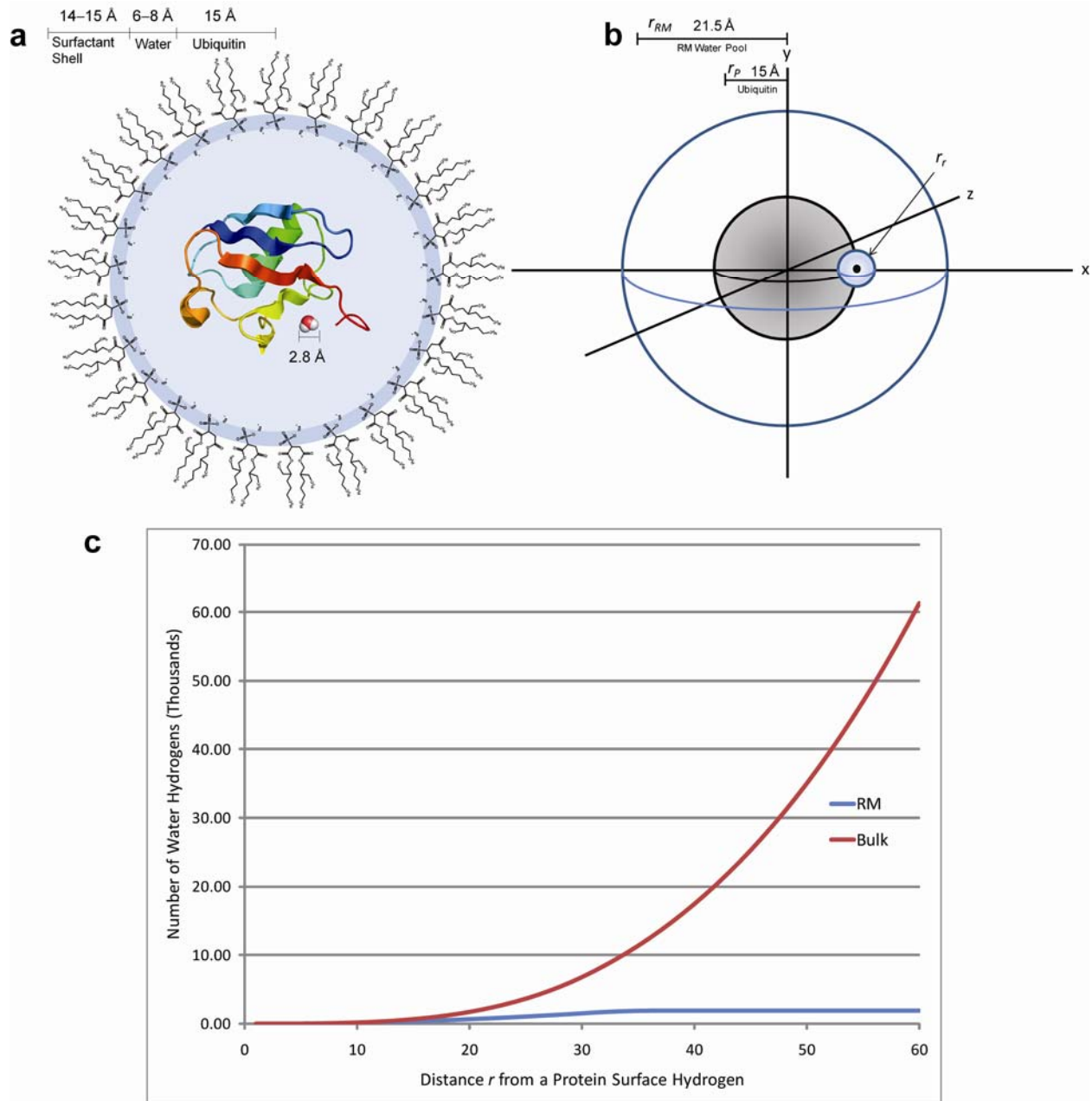
Correspondence should be addressed to A.J.W. (wand@mail.med.upenn.edu)



Supplementary Figure 1. Encapsulation results in slowed hydrogen exchange chemistry. ^{15}N -HSQC spectra of ubiquitin in reverse micelles (**a**) or aqueous solution (**b**). Overlaid spectra were obtained at pH 5 (blue), 5.5 (green), 6 (red), 6.5 (purple), 7 (orange), 7.5 (yellow), 8 (maroon), and 9 (black). The hydrogen exchange rate increases with increasing pH. As the hydrogen exchange rate approaches the difference in chemical shift between water and the amide hydrogen, the resonance will begin to broaden and as the pH is further increased will ultimately become unobservable. This provides a simple way to illustrate the rate of hydrogen exchange. The cross peak due to Gly 75 is highlighted to provide an example of a completely unprotected amide hydrogen whose intensity is therefore governed by the intrinsic hydrogen exchange chemistry. This peak is undetectable at $\text{pH} \geq 7$ in free aqueous solution while it remains detectable in reverse micelles. In reverse micelles, this cross peak is still observable even at pH 9. Contour levels in the pH 9 inset for the reverse micelle data (**b**) are lower than those shown in the full spectrum. These data demonstrate that fast hydrogen exchange chemistry is slowed in reverse micelles by approximately two orders of magnitude compared to bulk solution. Aqueous samples contained 1 mM ubiquitin, while 150 - 200 mM ubiquitin final concentration was used in reverse micelle samples. Reverse micelle samples were prepared using pH-adjusted AOT in pentane, and had $W_0 = 8.5\text{--}9.5$, as determined by ^1H NMR. For both aqueous and reverse micelle samples, the pH of the sample was confirmed using the pH-dependent ^1H chemical shifts of the buffers as internal NMR standards, acetate (pH 5–7) or imidazole (pH 7–9) ¹.

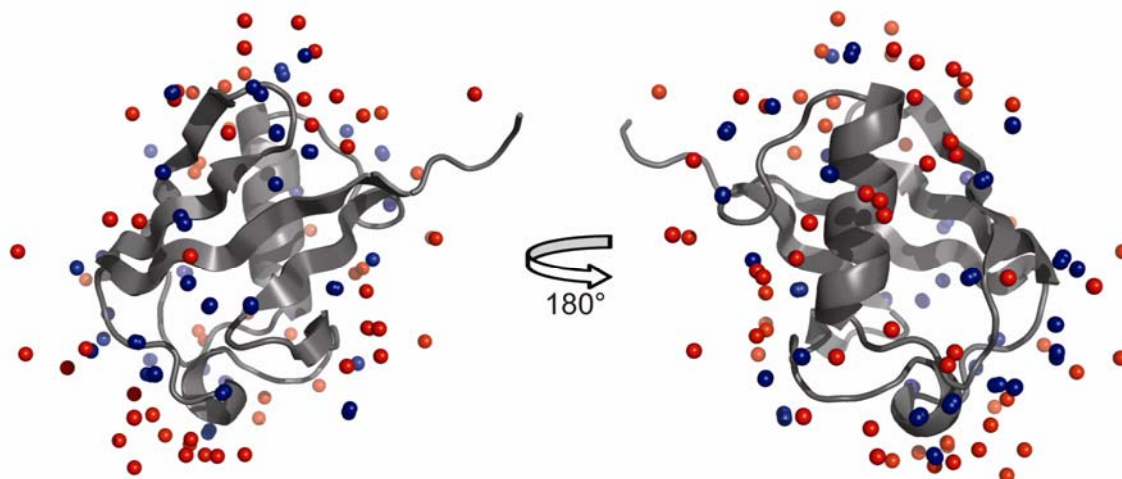


Supplementary Figure 2. Amide hydrogen cross peaks to hydroxyl hydrogens. Indirect ^1H strips of all resonances which show cross peaks to hydroxyl hydrogens are shown. The ROE data was used for this comparison in order to demonstrate that all detected cross peaks represent direct magnetization transfer, as indicated by the presence of negative ROE signals. The detected peaks are labeled according to the directly-detected amide peak (top) and indirect hydroxyl resonances (assigned at left). The cross peaks to Lys 6 and Leu 69 are tentatively assigned to a buried long-lived water molecule (H_2O_{II}) because these sites are more than 7 Å from any hydroxyl hydrogen. To be resolved in NMR spectra under reverse micellar conditions, hydroxyl groups must undergo hydrogen exchange chemistry with water at a rate slower than 1 s^{-1} , showing that hydroxyl hydrogen exchange is considerably slowed in the reverse micelle.



Supplementary Figure 3. Potential for long-range coupling of protein hydrogens to solvent hydrogens in RMs. **(a)** Schematic of ubiquitin in RM with the components of the system shown to-scale. **(b)** Diagram of the geometric conditions used to calculate **(c)** the number of water hydrogens within a given distance r_r of a surface-exposed protein hydrogen. The excluded volume of the protein, modeled as a rigid sphere, is included for both bulk solvation and RM

conditions. In the RM case, the surfactant layer, modeled as a rigid outer spherical boundary given by r_{RM} , excludes a majority of long-distance water as compared to the bulk solution condition. The number of water spins in the bulk case grows roughly as r_r^3 , whereas this value grows as roughly r_r^2 in the reverse micelle to a distance of ~ 35 Å, beyond which it remains constant because all of the RM water is within ~ 35 Å of any given surface protein hydrogen. The result is that long-range dipolar coupling of protein hydrogens to distant solvent hydrogens is minimized in the RM system.



Supplementary Figure 4. Variation of crystallographic waters. Ribbon diagram of PDB 1UBQ with the water molecules shown as well as the water molecules from PDB 1UBI overlaid. The water molecules that are within 1 Å between the two structures are colored blue, while the red water molecules are more than 1 Å from the nearest water in the other structure. Of the 58 waters in 1UBQ² and 81 waters in 1UBI³, 36 are common. The distances from each water oxygen, in both structures, to each amide hydrogen were calculated. Hydrogens were added in PyMOL⁴. For those amides which produced a cross peak to water in the reverse micelle spectra, the shortest amide-water distance for each was compared to the detection limit at 40 ms mixing time, ~ 4.3 Å $^1\text{H}-^1\text{H}$, which corresponds to ~ 5.2 Å $^1\text{H}_{\text{amide}} - \text{O}_{\text{water}}$ distance. Of the 54 amide-water interactions detected by NMR, more than half were outside this distance from any conserved crystallographic water. The NOE/ROE values were compared to the b-factors and occupancies of the nearest crystallographic waters, and no correlation was observed (data not shown).

Supplementary Table 1: $T_{1\rho}$ (± 0.0005 s) relaxation times for amides that show NOE and ROE cross peaks of opposite sign at the water resonance.

Residue	$T_{1\rho}$ (s)	Residue	$T_{1\rho}$ (s)	Residue	$T_{1\rho}$ (s)	Residue	$T_{1\rho}$ (s)
Gly 75	0.079	Thr 12	0.065	Thr 22	0.057	Ile 61	0.054
Gly 10	0.039	Thr 7	0.053	Leu 67	0.073	Ser 57	0.042
Leu 56	0.055	Val 70	0.057	Leu 71	0.059	Lys 11	0.035
Leu 50	0.067	Glu 18	0.075	Gln 41	0.044	Ile 3	0.060
Lys 63	0.081	Glu 64	0.057	Thr 66	0.062	Asn 25	0.030
Phe 4	0.071	Val 17	0.053	Asp 52	0.074	Ser 65	0.043
Arg 72	0.070	Leu 73	0.046	Arg 54	0.064	Asp 39	0.042
Asp 21	0.050	Thr 14	0.065	Leu 8	0.040	Asp 58	0.027
Asn 60	0.036	His 68	0.055	Gln 2	0.070	Thr 9	0.021
Arg 74	0.049	Lys 33	0.044	Ser 20	0.044	Gln 49	0.072
Asn 25 H ϵ	0.049	Leu 43	0.051	Thr 55	0.057		
Arg 42	0.052	Glu 16	0.077	Ala 46	0.058		
Leu 69	0.060	Leu 15	0.061	Gln 62	0.063		

Supplementary Table 2: NOE/ROE ratios (± 0.03) for amide hydrogens that showed a cross peak to water and were of sufficient resolution and signal-to-noise for quantitative analysis. Asterisks indicate ratios that were calculated using the maximum intensities rather than peak volumes due to weakness of the signal. ND indicates cross peaks that were too weak for quantitative analysis.

Residue	$\frac{NOE}{ROE}$	Residue	$\frac{NOE}{ROE}$	Residue	$\frac{NOE}{ROE}$	Residue	$\frac{NOE}{ROE}$
Gly 75	-0.53	Thr 7	-0.46	Leu 71	-0.36	Ile 3	-0.26
Gly 10	-0.52	Val 70	-0.45	Gln 41	-0.36	Asn 25	-0.25
Leu 56	-0.51	Glu 18	-0.42	Thr 66	-0.35	Ser 65	-0.23
Leu 50	-0.51	Glu 64	-0.42*	Asp 52	-0.34	Asp 39	-0.22
Lys 63	-0.50	Val 17	-0.42	Arg 54	-0.34*	Asp 58	-0.19
Phe 4	-0.50	Leu 73	-0.42	Leu 8	-0.32	Thr 9	-0.14
Arg 72	-0.50	Thr 14	-0.41	Gln 2	-0.32	Gln 49	-0.07
Asp 21	-0.50	His 68	-0.40	Ser 20	-0.31	Lys 6	ND
Asn 60	-0.49	Lys 33	-0.40	Thr 55	-0.30	Ile 23	ND
Arg 74	-0.49	Leu 43	-0.40	Ala 46	-0.30	Ile 44	ND
Asn 25 H ϵ	-0.48	Glu 16	-0.40	Gln 62	-0.30	Gly 76	ND
Arg 42	-0.48*	Leu 15	-0.39	Ile 61	-0.28*		
Leu 69	-0.47	Thr 22	-0.39	Ser 57	-0.27		
Thr 12	-0.47	Leu 67	-0.37	Lys 11	-0.26		

1. Baryshnikova, O.K., Williams, T.C. & Sykes, B.D. Internal pH indicators for biomolecular NMR. *J. Biomol. NMR* **41**, 5-7 (2008).
2. Vijay-Kumar, S., Bugg, C.E. & Cook, W.J. Structure of ubiquitin refined at 1.8 Å resolution. *J. Mol. Biol.* **194**, 531-44 (1987).
3. Alexeev, D. et al. Synthetic, structural and biological studies of the ubiquitin system: chemically synthesized and native ubiquitin fold into identical three-dimensional structures. *Biochem. J.* **299**, 159-63 (1994).
4. DeLano, W.L. The PyMOL molecular graphics system. (DeLano Scientific LLC, Palo Alto, California, USA, 2009).